Mechanical Properties of a Mackinawite Corrosion Product Layer

Ezechukwu Anyanwu, Claudia Prieto, Bruce Brown, Marc Singer
Institute for Corrosion and Multiphase Technology, Ohio University
342 West State Street
Athens, OH, 45701
USA

Mechanical properties of the corrosion product layers as well as corrosion mechanisms need to be studied for better prediction of general and localized corrosion and to develop a holistic understanding of corrosion mechanisms in upstream oil and gas pipelines. Various ongoing research efforts have focused on the topic of sour corrosion mechanisms, while minimal attention has been paid to ascertaining the mechanical properties of the iron sulfide layers developed in these environments. The effects of fluid flow (i.e. erosion/corrosion, wall shear stress) as well as the impact of different operations (i.e. wellbore cleaning, wireline tools) on the internal pipeline wall, may lead to partial removal of corrosion product layers. This is an important topic, since mechanical damage of protective iron sulfide layers may lead to localized corrosion. To investigate the magnitude of stress required to damage iron sulfide layers up to the point of exposing the substrate, well-defined iron sulfide layers were developed in a 4-liter glass cell and the mechanical properties of the layers, such as hardness and adhesive strength, were investigated using a mechanical tester. To develop the iron sulfide layer, UNS G10180 carbon steel specimens were exposed to a 1 wt.% NaCl solution at pH of 6.0, and 0.1bar H_2S (in a mixture with N_2). FeS layers were developed at two solution temperatures, 30°C and 80°C, and the hardness and interfacial shear strength of the layers formed after 1 day and 3 days of exposure were investigated. The morphological characteristics of the FeS layers under investigation were examined by conducting SEM and cross-sectional analysis. XRD analysis confirmed mackinawite as the phase of the iron sulfide layer. While the interfacial shear strength of this mackinawite layer was found to be 5 magnitudes higher than the maximum flow related shear stress typically encountered in oil and gas operations, the integrity may still be compromised if these layers are subjected to other mechanical impacts (cavitation, droplet impingement) that may occur during production.

Key words: Iron sulfide, mackinawite, shear stress, mechanical property, hardness, adhesive strength.

Symposium: TEG 282X Sour Corrosion.

INTRODUCTION

The integrity management of oil and gas pipelines is usually associated with the control of corrosion threats which occur as a result of the production processes. While many studies have focused on understanding the chemical/electrochemical aspects of corrosion mechanisms associated with the transport of produced fluids,[1–4] little attention has been given to the mechanical properties of scales or corrosion products forming on the pipe surface. These layers are constantly exposed to stresses generated by fluid flow, and other dynamic events (cavitation, droplet impingement), which may lead to their partial removal. The mechanical damage of iron carbonate or iron sulfide, typically encountered in oil and gas production, increases the likelihood of occurrence of localized corrosion. It is therefore critical to understand their mechanical properties. Studies have been conducted to evaluate the ability of $FeCO_3$ to withstand typical flow related wall shear stresses as it occurs in the field,[5–7] but similar studies have not been done for FeS layers until now.

Different methods have been used by researchers to determine the stress required to remove an iron carbonate layer. Modified tensile test experiments have been performed,[7] where the iron carbonate layer was detached from the surface by an applied tensile force normal to the substrate surface. These experiments used epoxy to attach to an iron carbonate layer and test for layer detachment over an area of the order of $1cm^2$. Another method used atomic force microscopy to apply a shear force of the order of nanonewtons on an individual iron carbonate crystal with the intent to cause full detachment.[5] The reported shear stress required to remove iron carbonate layer in both cases was of the order of 10^6 Pa, which is 3 orders of magnitude higher than the maximum flow related wall shear stress typically encountered in a multiphase pipe flow[6]. Even though both methods involved pre-formed iron carbonate layers in ex-situ conditions to evaluate the shear stress values, these results, when extrapolated to $FeCO_3$ layers formed in production conditions, show clearly that flow related shear stresses in pipelines are not sufficient to generate damage. Similar studies have not yet been conducted on iron sulfide layers probably because of the complexity of corrosion product layers formed in sour environment.

The aim of the current study was to investigate the magnitude of shear stress required to damage an iron sulfide layer up to the point of exposing the substrate. To achieve this research goal, a well-defined iron sulfide layer developed under controlled conditions was tested for its mechanical properties using a mechanical scratch tester. Indentation measurements and scratch test were used to determine the hardness and interfacial shear strength of a pre-formed iron sulfide layer.

An indentation measurement involves the application of a load by an indenter in contact with a specimen and the subsequent removal of this load when the preset force is reached.[8,9] Figure 1 shows a typical elastic-plastic loading and elastic unloading curve from an indentation measurement. The hardness of the material is determined by dividing the load by the impressed area on the substrate.
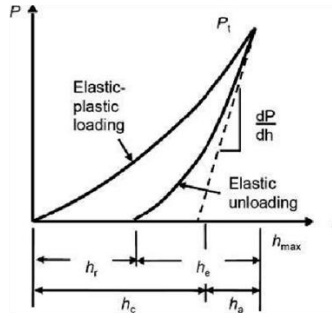
Figure 1: A typical loading and unloading curve from an indentation test[8]

The impressed area, also known as the projected area, can be calculated from the penetration depth of the indenter. The projected area shown in Equation (1) is dependent on the indenter shape that is used and is calculated by the expression in Equation (2).

$$H = \frac{P}{A_{Proj}}$$ (1)

Where P is the maximum load and A_{proj} is the projected area.

For the current studies, a Vickers indenter, shown Figure 2, was used for all the hardness measurements and the projected areas can be calculated using Equation (2) below.[8]
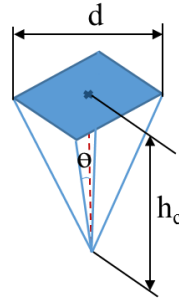

Figure 2: A schematic of a Vickers indenter tip with dimensions

$$A_{Proj} = 24.5h_c^2$$ (2)

Where h_c, is the effective height of the indenter.

Scratch Test

A scratch test involves the movement of an indenter tip across a surface it is in contact with and the determination of possible failure modes and characteristics. A scratch test can be either progressive or constant. For a progressive load scratch test, the indenter is moved across the surface with a linearly increasing normal force until failure occurs at critical load (CL). In contrast, a constant load test involves the movement of an indenter tip across a surface while maintaining the normal force at a constant level. The progressive load scratch test is appropriate for obtaining an estimated range of force for the occurrence of failure. The actual CL can be determined from constant load tests, by conducting scratch tests at different constant loads within the range of forces established by the progressive load test.

Modes of Failure during Scratch Testing

The failure mode that occurs during a scratch test can be either cohesive or adhesive.[10,11] Cohesive failure occurs within the layer while an adhesive failure occurs at the layer-substrate interface where there is a separation of the layer from the surface either by cracking or by full separation. The different types of cohesive failure are, chevron, arc tensile, Hertzian and conformal cracks while an adhesive failure can occur in the form of buckling, wedging, recovery and gross spallation. The dependence of the above mentioned types of failure on the layer and substrates hardness have been discussed elsewhere.[11]

Shear Stress Calculation from Scratch Test Measurements

Early models[12,13] used the hardness of the substrate, obtained from indentation measurements, to calculate the interfacial shear strength of the layer. Equations 3 - 5 shows the expressions for calculating the shear stresses with parameters from Figure 3 which illustrates of an indenter tip with the different forces acting on it during scratch test.
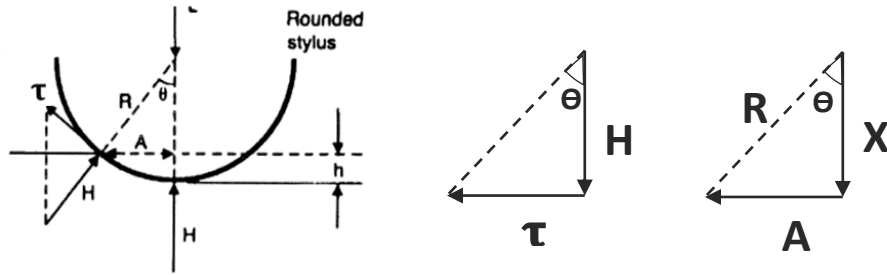

Figure 3: Schematics of the forces and dimensions associated with a stylus tip in contact with a surface during a scratch test.

$$\tau = H \tan \theta \tag{3}$$

$$\tan \theta = \frac{A}{\sqrt{R^2 - A^2}} \tag{4}$$

$$\tau = \frac{AH}{\sqrt{R^2 - A^2}} \tag{5}$$

Where, τ is the shear stress in Pa, H is the substrate hardness in Pa, R is the indenter radius in meters, A is half width of the scratch track in meters, θ is the angle of friction in degrees and X is an introduced variable used for calculation (in m).

An improved shear stress calculation model developed by Ollivier, *et al.,*[14] uses the critical load from a scratch test to determine the interfacial shear strength. This new model replaces the hardness of the substrate, H, in Equation 5 with $L_c/\pi A^2$, as shown in Equation 6.[14]

$$\tau = \frac{L_c}{\pi A \sqrt{R^2 - A^2}} \tag{6}$$

Where L_c (Pa) is the critical load for the occurrence of a failure.

This model has been shown to be more accurate than the Benjamin and Weaver model[14] and this was used for all the shear stress evaluations in the current study.

Experimental Method

Iron Sulfide Layer Development

Iron sulfide layers were developed in a 4-liter glass cell, under controlled chemistry and mass transfer conditions and the mechanical properties of the layers, such as hardness and adhesive strength, were investigated using a mechanical tester. The glass cell test setup (Figure 4) accommodates up to seven 0.5" x 0.5" x 0.1" square specimen mounted on holders and has an impeller at the center to simulate controlled flowing conditions. The 4-litre glass cell setup was designed so that specimen holders could be inserted or removed during testing without disrupting the test environment. In growing the iron sulfide layer, UNS G1018 carbon steel specimens were inserted in 1 wt.% NaCl solution saturated with 0.1bar H_2S in a mixture with nitrogen at pH of 6.0. Before inserting the samples, the solution was deoxygenated by sparging with N_2 for two hours. H_2S was introduced into the inlet gas stream to achieve and H_2S partial pressure of 0.1bar at the different temperatures (10% vol. H_2S/nitrogen gas mixture at 30°C and 19% vol. H_2S/nitrogen gas mixture at 30°C). The solution was sparged with this gas stream for an additional 30 minutes while the impeller rotation was set at the desired speed. Solution temperature was maintained at the desired value and pH was adjusted to 6.0 with deoxygenated 1M NaOH solution. The carbon steel specimens were polished with a silicon carbide papers in the order 150 grit, 400 grit and 600 grit. Specimens were cleaned by putting them in a beaker containing isopropanol and placed in an ultrasonicator for 5 minutes. Six specimens were individually inserted and exposed in each experiment. At the time of extraction, specimen holders were individually withdrawn from the solution and specimens were carefully removed while preserving the corrosion product layer. Each extracted specimen was dipped in a beaker of deoxygenated deionized water to remove salts, dipped in a beaker of isopropanol to remove the water and then dried in a vacuum desiccator. Three specimens were extracted after 1 day and three specimens were extracted after 3 days. All extracted specimens were immediately stored in a vacuum desiccator for further analysis. For the three specimens extracted on each stipulated day, SEM and cross-sectional analyses were conducted on one, adhesive strength tests on the second, and hardness measurements on the third. XRD analysis was only conducted on a sample extracted after 3 days exposure time. For these experiments, FeS layers were developed at two temperatures, 30°C and 80°C, in order to investigate the impact of temperature on the mechanical properties of these layers.

Equipment:

The FeS layers were developed in a 4-liter glass cell with impeller shown in Figure 4. This system provides a good control of the solution chemistry and the mass transport of species.[15] For this set of experiments, the iron sulfide layer was developed at the 250 rpm rotational speed, which corresponds to Fe^{2+} and H_2S mass transfer coefficient of 6.8 x 10^{-5}m/s and 1.2 x 10^{-4}m/s, respectively.
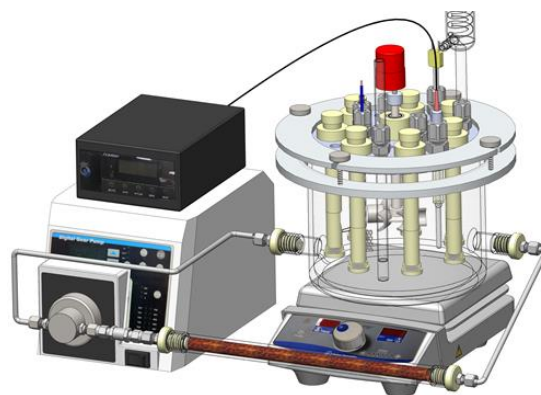
Figure 4: Glass Cell with specimen holder, impeller assembly and water chemistry control system

Mechanical Testing

The hardness of a UNS G10180 carbon steel was measured by conducting an indentation measurement at maximum force of 300mN. Indentation measurements were also conducted on the FeS layers developed at solution temperatures of 30°C and 80°C after 1 and 3 days exposure periods. Afterwards, a progressive load test was conducted on the specimens with corrosion product layers from 0.1mN to 300mN at a loading rate of 75mN/min, a scratch speed of 0.25mm/min and a scratch length of 1mm. The scratched specimen was examined under the SEM for the occurrence of the adhesive failure. After the detection of the adhesive failure, a constant load test was conducted to determine the critical load (CL) for the adhesive failure of the FeS layer.

Equipment:

The mechanical properties of the FeS layers developed in the glass cell were investigated using the Nanovea+ CB500 mechanical tester.[16] This system can be used to perform a hardness measurement and a scratch adhesion tests in the range of forces between 0.1mN to 800mN. The three indenters which can be used in this system are the conical, Berkovich and Vickers indenter. The tip of these indenters have different shapes which makes them suitable for a variety of mechanical tests.[17] The conical indenter is suitable for scratch tests only, while the Berkovich and Vickers indenter are suitable for indentation measurements.[11]

Material Tested

The material used for the current studies is a UNS G10180 and the chemical composition of this material is shown in Table I.

Table I: The percentage chemical composition of UNS G10180 carbon steel

UNS G10180 mild steel (balance Fe) in wt. %									
Al	**As**	**C**	**Co**	**Cr**	**Cu**	**Mn**	**Mo**	**Nb**	**Ni**
0.001	0.007	0.160	0.010	0.063	0.250	0.790	0.020	0.006	0.078
P	**S**	**Sb**	**Si**	**Sn**	**Ti**	**V**	**Zr**		
0.008	0.029	0.011	0.250	0.017	<0.001	0.001	0.004		

Test Matrix:

Table II shows the test matrix for the development of FeS layers and the subsequent testing of the mechanical properties.

Table II:Test Matrix

Operating Parameter	Specification
Material	UNS G10180
H_2S Partial Pressure	0.1 bar
Total Pressure	1.01 bar
Electrolyte	1 wt.% NaCl
Solution pH	6.0
Temperature	30^0C, 80^0C
Impeller Rotational Speed	250rpm
Exposure Time	24 & 72hrs
Mechanical Testing Technique	Hardness, Progressive Load Test, Constant Load Tests
Surface Analysis	SEM, EDS, XRD

Results and Discussion

Characterization of FeS layer

The SEM analysis of specimen surface after 1 day and 3 days exposure to the corrosive environment at different temperatures (30°C and 80°C) are shown in Figure 5.
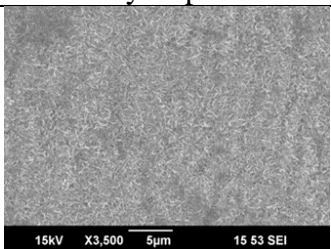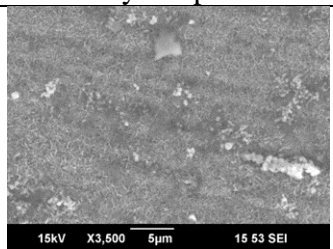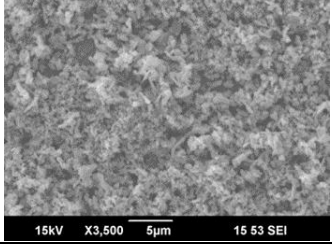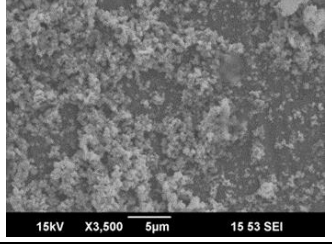
Test Condition	1 Day Exposure	3 Days Exposure
H_2S Partial Pressure = 0.1bar Total Pressure = 1.01 bar Electrolyte = 1wt.% NaCl Solution pH = 6.00 Temperature = 30^0C Impeller Speed = 250rpm		
H_2S Partial Pressure = 0.1bar Total Pressure = 1.01 bar Electrolyte = 1wt.% NaCl Solution pH = 6.00 Temperature = 80^0C Impeller Speed = 250rpm		

Figure 5: Surface SEM of FeS layer formed on UNS G10180 at different exposure times and temperatures.

The SEM analysis of sample surface presented in Figure 5 shows that the exposure time did not play a role in the morphology of the FeS layers at the respective temperatures. These surface SEM images,

especially those formed at 80°C, show two distinct layers, an outer fluffy FeS layer and an inner compact FeS layer. The two layer structure of the FeS layers is confirmed from the cross section of the layers presented in Figure 6.

Test Condition	1 Day Exposure	3 Days Exposure
H$_2$S Partial Pressure = 0.1bar Total Pressure = 1.01 bar Electrolyte = 1wt.% NaCl Solution pH = 6.00 Temperature = 30^{0}C Impeller Speed = 250rpm		
H$_2$S Partial Pressure = 0.1bar Total Pressure = 1.01 bar Electrolyte = 1wt.% NaCl Solution pH = 6.00 Temperature = 80^{0}C Impeller Speed = 250rpm		

Figure 6: Cross section of FeS layer formed on UNS G10180 at different exposure times and temperatures.

The outer fluffy layer that forms at 80°C appears to be more porous and loosely attached than that formed at 30°C. Ning, *et al.,*[18] developed FeS layers of similar morphology under the conditions at 80°C. It was reported that the corrosion rates under these conditions decreased from an initial value of 1.1mm/year to 0.07mm/year indicating these layers are protective. The thickness of the FeS layers formed at 30°C and 80°C were approximately 2.3±0.14µm and 2.85±0.3µm, respectively.

The phase of FeS layers was confirmed as mackinawite from the XRD analysis presented in Figure 24. This shows that iron sulfide of the same phase can possess different morphological characteristics.
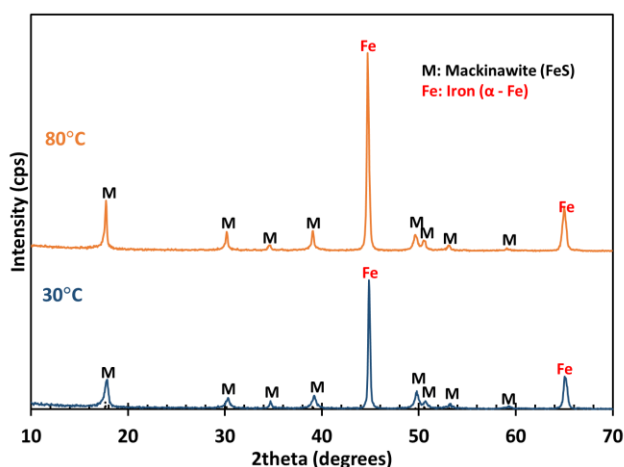

Figure 7: XRD analysis of FeS layer formed on UNS G10180 after 3 days exposure to 1 wt.% solution at pH 6.0, 250rpm impeller rotation speed and different temperatures (30°C and 80°C).

Hardness Measurement of Substrate and Layers

The hardness values from nanoindentation measurements conducted on a bare UNS G10180 carbon steel and on the mackinawite layers formed at the different temperatures and specimen exposure are presented in Table III. All indentation measurements were conducted with a Vickers indenter.

Table III: Summary of hardness measurements of bare UNS G10180 carbon steel and mackinawite layers formed at different temperatures and exposure time

Material	Hardness
Bare UNS G10180 carbon steel	3.78 ± 0.23GPa (357 ± 21.43HV)
Mackinawite layer formed after 1 day in 30°C solution	0.30 ± 0.12GPa (28.40 ± 11.90HV)
Mackinawite layer formed after 3 day in 30°C solution	0.40 ± 0.04GPa (38.30 ± 4.30HV)
Mackinawite layer formed after 1 day in 80°C solution	0.03 ± 0.01GPa (2.90 ± 0.58HV)
Mackinawite layer formed after 3 day in 80°C solution	0.08 ± 0.01GPa (7.60 ± 1.30HV)

The average hardness value of UNS G10180 mild steel agrees with the findings from the studies carried out by Jian, *et al.,*[19] where a Vickers hardness of 330HV was reported for the same substrate. Since the hardness values of the substrates are more than 13 times higher than that of the mackinawite layers, the expected mode of cohesive failure for this layer is conformal cracking, while spallation or buckling would be indicative of an adhesive failure.[11] The tracks from scratch tests were inspected to ascertain the occurrence of these modes of failures.

Progressive Load Test on Mackinawite Layers formed on UNS G10180 after 1 day Exposure

Studies have shown similarities in the hardness measurements conducted with conical and Vickers indenters, in contrast to the large variation in results when conical indenters are compared to those from Berkovich intenders[17]. Therefore, to have better correlation of hardness measurements (conducted with a Vickers indenter) and scratch test results, the conical indenter was used to conduct all the scratch tests. Figure 8 shows a typical scratch track from a progressive load test on the mackinawite layer.
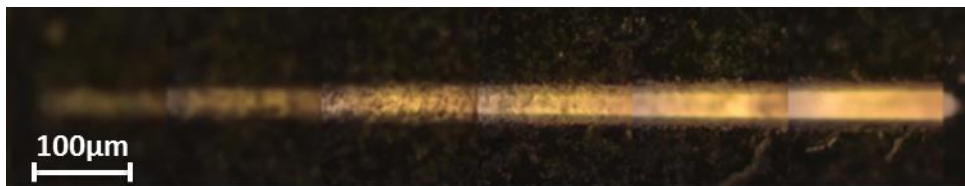

Figure 8: Progressive load scratch track from 0.1mN to 300mN on the mackinawite layer formed in 30°C solution after 1 day, conducted at a scratch speed of 0.25mm/min and loading rate of 75mN/min.

Since the force loading rate is linear, the range of force where an adhesive failure occurred was identified by inspecting the beginning, the middle and the end of the scratch track, corresponding to the minimum (0.1mN), median (150mN) and maximum (300mN) load. In addition to direct observation of changes in the contraction between areas with different forms of failure, the occurrence an adhesive failure was confirmed by energy-dispersive X-ray spectroscopy (EDS) technique. Table IV and Table V shows the summary of the EDS spot analyses on sections of the scratch tracks from progressive load tests conducted on the mackinawite layer formed at 30°C and 80°C, respectively.

Table IV: Summary of EDS analyses on sections of progressive load scratch track corresponding to 0.1mN, 150mN and 300mN normal forces. (Mackinawite layers formed after 1 day exposure of UNS G10180 to 1 wt.% solution at pH 6.0, 0.1mbar H_2S in N_2, 30°C, and 250rpm impeller speed)
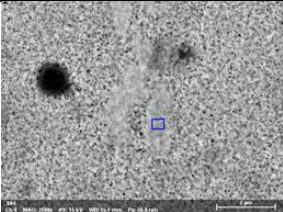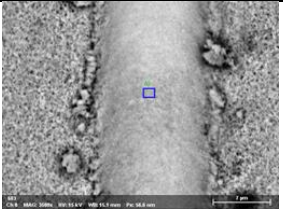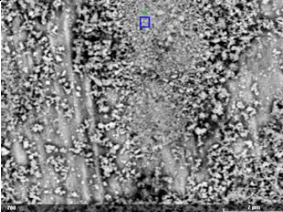
	0.1mN		150mN		300mN	
Sections of scratch track from progressive load test						
Atom percentage from EDS spot analyses	**Element**	**Atom %**	**Element**	**Atom %**	**Element**	**Atom %**
	Iron	**50.46**	**Iron**	**49.15**	**Iron**	**73.59**
	Sulfur	**42.33**	**Sulfur**	**41.07**	**Sulfur**	**21.32**
	Oxygen	7.20	Oxygen	9.78	Oxygen	5.09
Form of failure	Cohesive Failure		Cohesive Failure		Adhesive Failure	

Table V: Summary of EDS analyses on sections of progressive load scratch track corresponding to 0.1mN, 150mN and 300mN normal forces. (Mackinawite layers formed after 1 day exposure of UNS G10180 to 1 wt.% solution at pH 6.0, 0.1mbar H_2S in N_2, 80°C, and 250rpm impeller speed
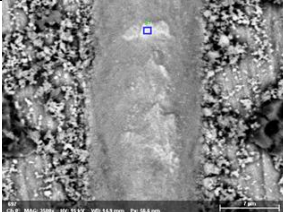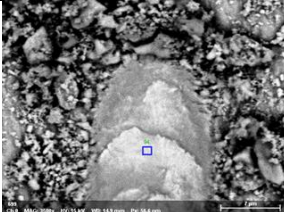
	0.1mN		150mN		300mN	
Sections of scratch track from progressive load test						
Atom percentage from EDS spot analyses	**Element**	**Atom %**	**Element**	**Atom %**	**Element**	**Atom %**
	Iron	**52.29**	**Iron**	**78.76**	**Iron**	**88.26**
	Sulfur	**45.32**	**Sulfur**	**17.65**	**Sulfur**	**9.72**
	Oxygen	2.39	Oxygen	3.59	Oxygen	2.01
Form of failure	Cohesive Failure		Adhesive Failure		Adhesive Failure	

Table IV shows a high iron to sulfur atom % ratio at maximum load of 300mN while an approximately equal iron and sulfur atom % ratio was detected at 150mN and 0.1mN indicating a critical load for adhesive failure between 150 and 300mN. In contrast, the EDS analyses of the progressive load scratch track on the mackinawite layer formed at 80°C (Table V) shows a high iron to sulfur atom % ratio at 300mN and 150mN and an approximately equal iron to sulfur atom % ratio at 0.1mN. This suggests that the critical load for the occurrence of adhesive failure is between 0.1mN and 150mN. It was assumed that the critical load for adhesive failure of the FeS layer formed after 3 days would be within the same range of force since the layer thickness and hardness were similar in magnitude to those layers formed after 1 day.

Constant Load Test on Mackinawite Layers Formed on UNS G10180 after 1-day Exposure

A cohesive form of failure occurred on the mackinawite layers formed at 30°C and 80°C from constant load tests conducted at normal force of 200mN and 100mN, respectively (Figure 9). The scratch speed was set at the same value as the progressive load test, 0.25mm/min.
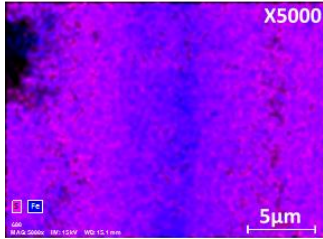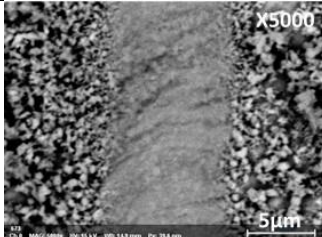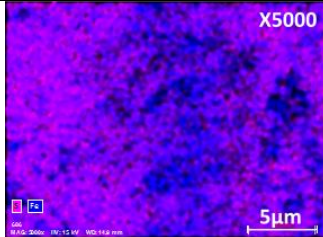
Test Condition	Scratch Track	EDS Mapping
H_2S Partial Pressure = 0.1bar Total Pressure = 1.01 bar Electrolyte = 1wt.% NaCl Solution pH = 6.00 Temperature = 30°C Normal Force = 200mN		
H_2S Partial Pressure = 0.1bar Total Pressure = 1.01 bar Electrolyte = 1wt.% NaCl Solution pH = 6.00 Temperature = 80°C Normal Force = 100mN		

Figure 9: EDS mapping of a cohesive scratch failure on mackinawite layers formed after 1 day exposure at different temperatures

The EDS mapping presented in Figure 9 shows areas of slightly high iron intensity. However, the back scatter image shows a relatively uniform contrast, which would not be the case if the substrate metal were exposed. Therefore, the evidence was not strong enough to conclude that adhesive failure occurred.

However, the EDS mapping of the scratch produced by a load of 230mN and 150mN on the mackinawite layers formed at 30°C and 80°C, respectively (Figure 10) showed distinct areas with higher Fe intensities. Additionally, the backscatter analysis of the scratch mark at this force shows areas of different contrasts which also corresponds to the areas of higher Fe intensity on the EDS map. This evidence is strong enough to conclude that an adhesive failure of the FeS layer occurred.
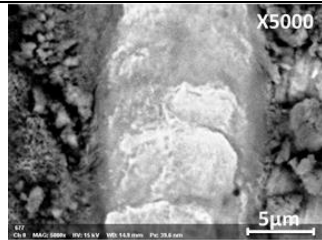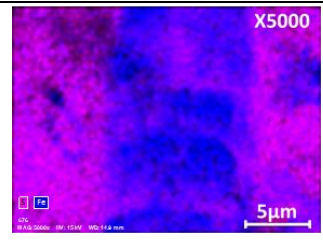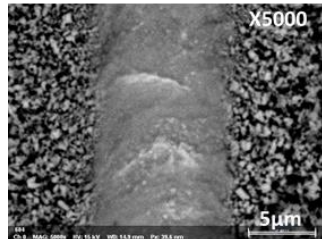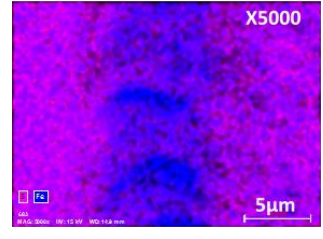
Test Condition	Scratch Track	EDS Mapping
H_2S Partial Pressure = 0.1bar Total Pressure = 1.01 bar Electrolyte = 1wt.% NaCl Solution pH = 6.00 Temperature = 30°C Normal Force = 230mN		
H_2S Partial Pressure = 0.1bar Total Pressure = 1.01 bar Electrolyte = 1wt.% NaCl Solution pH = 6.00 Temperature = 80°C Normal Force = 150mN		

Figure 10: EDS mapping of an adhesive scratch failure on mackinawite layers formed after 1 day exposure at different temperatures

An important parameter in the Benjamin and Weaver model[12] for calculation of the interfacial shear strength is the scratch width. The scratch width on the mackinawite developed at 30°C was

approximately 18µm, while that from the 150mN constant load test on the mackinawite formed at 80°C was approximately 12µm. These correspond to interfacial shear stresses of 470MPa for the layer formed at 30°C and 410MPa for the layer formed at 80°C.

The profilometry of the scratched areas presented in Figure 11 showed that the depth of the scratch mark resulting from 470 MPa and 410 MPa shear stress was 2.3 µm and 3.0 µm, respectively.
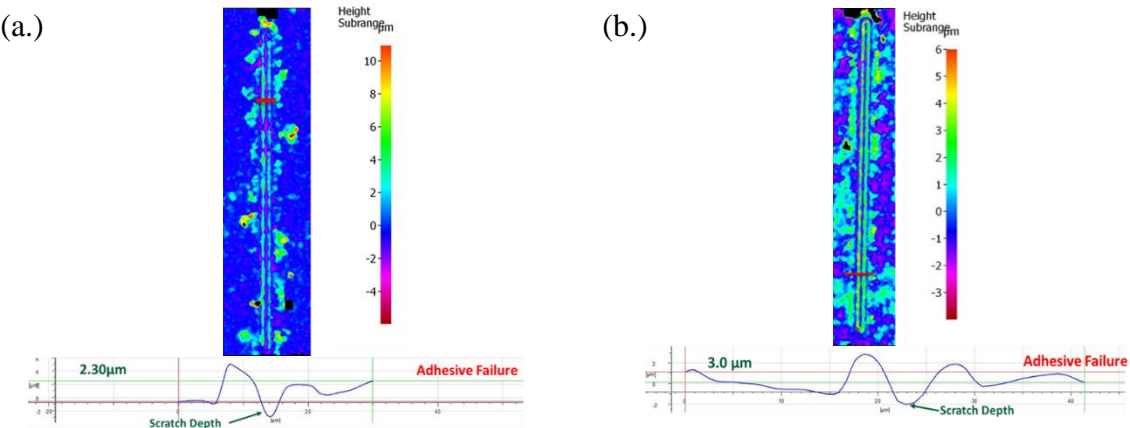

Figure 11: Profilometry of the scratched areas from a shear stress of (a.) 470 MPa on the mackinawite layer formed at 30°C and (b.) 410 MPa on the mackinawite layer formed at 80°C after 1 day

The scratch depths agree with the measured layer thickness presented in Figure 6, which confirms that adhesive failure occurred at the layer/substrate interface.

Constant Load Test of Mackinawite Layer Formed on UNS G10180 after 3 days Exposure

The critical load for the adhesive failure of mackinawite layers developed at 30°C and 80°C after 3 days is 250mN and 150mN, respectively. This was confirmed by the EDS mapping of the scratch mark presented in Figure 12.

Test Condition	Scratch Track	EDS Mapping
H_2S Partial Pressure = 0.1bar Total Pressure = 1.01 bar Electrolyte = 1wt.% NaCl Solution pH = 6.00 Temperature = 30°C Normal Force = 250mN		
H_2S Partial Pressure = 0.1bar Total Pressure = 1.01 bar Electrolyte = 1wt.% NaCl Solution pH = 6.00 Temperature = 80°C Normal Force = 150mN		

Figure 12: EDS mapping of an adhesive scratch failure on mackinawite layers formed after 3 days exposure at different temperatures

The calculated interfacial shear strength of the mackinawite layers formed at 30°C (scratch width, 2A ≈ 18µm, Lc = 250mN) and 80°C (scratch width, 2A ≈ 14µm, Lc = 150mN) was 500MPa and 370MPa, respectively.
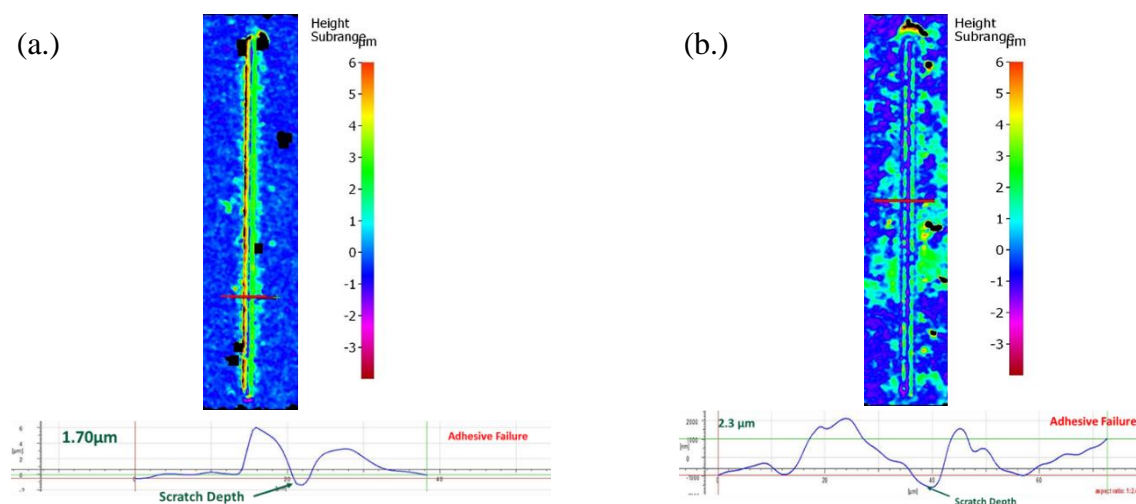
(a.)

(b.)

Figure 13: Profilometry of the scratched areas from a shear stress of (a.) 500 MPa on the mackinawite layer formed at 30°C and (b.) 370MPa on the mackinawite layer formed at 80°C after 3 day

Figure 13 shows that the depth of the scratch track associated with the adhesive failures of the mackinawite layers formed at the respective temperatures were 1.7 µm and 2.3 µm confirming that adhesive failure occurred at the layer/substrate interface.

The summary from the mechanical testing of the mackinawite layers formed on UNS G10180 at different exposure times and temperatures are presented in Table VI.

Table VI: Summary of results obtained for mechanical characterization of mackinawite layer formed at different exposure times and temperature.

Exposure Time	Operating Temperature	FeS Layer Hardness	Critical Load	Scratch Depth	Interfacial Shear of Inner Mackinawite Layer
1 Day	30°C	0.30 GPa	230mN	2.3µm	0.47 GPa
	80°C	0.03 GPa	150mN	3.0µm	0.41 GPa
3 Days	30°C	0.40 GPa	250mN	1.7µm	0.50 GPa
	80°C	0.08 GPa	150mN	2.3µm	0.37 GPa

Conclusions

The mechanical properties mackinawite corrosion product layers formed on UNS G10180, at 30°C and 80°C, pH 6, 0.1bar H_2S (in a mixture with N_2) and considering exposure times of 1 and 3 days, were investigated using hardness and scratch tests measurements. The mode of adhesive failure obtained for all the layers tested was buckling. The mode of cohesive failure expected was conformal cracking considering the hardness of the layers and the substrate. While this mode of cohesive failure was evident for the scratches in layers formed at higher temperature, the appearance of conformal cracks was less pronounced in the layer formed at lower temperature. This may be due to the fact that the layers formed at 80°C had a lower hardness than those formed at 30°C, which is more favorable for the formation of conformal cracks.

The chart presented in Figure 14 shows the interfacial shear strength of the different layers tested while the red line on the chart shows the maximum wall shear stress that can be generated by flow alone. Furthermore, the calculated interfacial shear strength suggests that the adhesive force of the layer formed at 80°C was less than that of the layer formed at 30°C. This finding agrees with the studies conducted by Zheng, *et al.,* where it was reported that a denser but weakly attached FeS layers formed at higher temperature H_2S environments in comparison to a lower temperature environment [14].
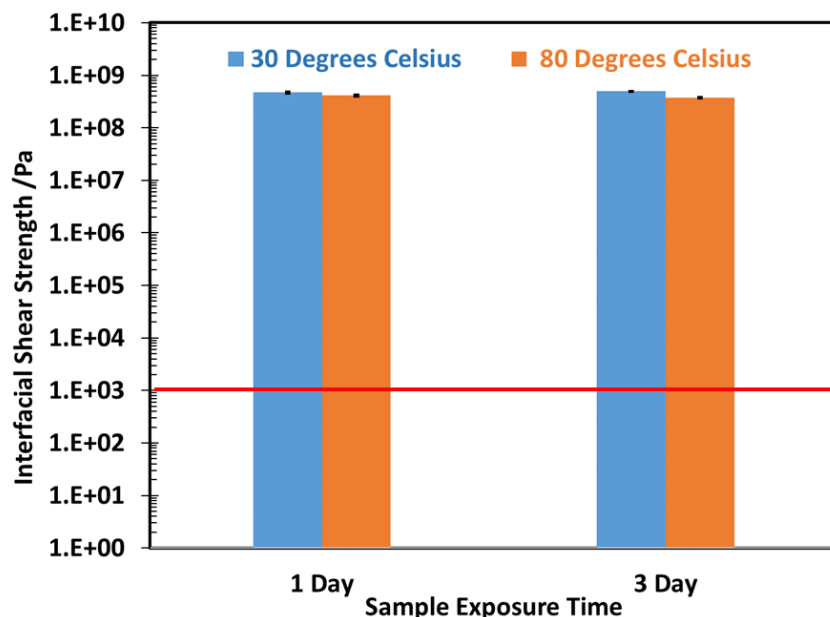

Figure 14: Summary of the interfacial shear strength of mackinawite layers formed in 30^0C and 80^0C solutions compared to the highest possible flow related shear stress in pipelines.

The following conclusions were reached based on these results:

- The inner mackinawite layer would require a shear stress on the order of 10^8Pa magnitude to remove. This is two orders of magnitude higher than the lateral stress required to remove an iron carbonate layer[5].
- The typical shear stress in oil and gas pipelines is 5 magnitudes less than the stress values required to remove the inner mackinawite layers.

Acknowledgements

References

[1]   Y. Zheng, J. Ning, B. Brown, D. Young, and S. Nesic, "Mechanistic study of the effect of iron sulfide layers on hydrogen sulfide corrosion of carbon steel," *CORROSION/2015*, paper no. 5933 (Dallas, TX: NACE 2015).

[2]   S. Nesic, Y. Zheng, B. Brown, and J. Ning, "Advancement in predictive modeling of mild steel corrosion in CO_2 and H_2S containing environments," *CORROSION/2015*, paper no. 6146 (Dallas, TX: NACE 2015).

[3]   S. Nesic, J. Postlethwaite, and S. Olsen, "An Electrochemical Model for Prediction of Corrosion of Mild Steel in Aqueous Carbon Dioxide Solutions," *Corrosion* 52 (1996), pp. 280–294.

[4]   W. Sun, S. Nešić, and S. Papavinasam, "Kinetics of Iron Sulfide and Mixed Iron Sulfide/Carbonate Scale Precipitation in CO_2/H_2S Corrosion," *CORROSION/2006, paper* no. 6644 (San Diego, CA: NACE 2006).

[5]   W. Li, Y. Xiong, B. Brown, K. E. Kee, and S. Nesic, "Measurement of Wall Shear Stress in Multiphase Flow and Its Effect on Protective FeCO3 Corrosion Product Layer Removal," *CORROSION/2015*, paper no. 5922 (Dallas, TX: NACE 2015).

[6]   W. Li, B. F. M. Pots, B. Brown, K. E. Kee, and S. Nesic, "A direct measurement of wall shear stress in multiphase flow-Is it an important parameter in CO_2 corrosion of carbon steel pipelines?," *Corros. Sci.*, vol. 110, pp. 35–45, 2016.

[7]   Y. Yang, B. Brown, S. Nešić, M. E. Gennaro, and B. Molinas, "Mechanical strength and removal of a protective iron carbonate layer formed on mild steel in CO_2 corrosion," *CORROSION/2010*, paper no. 10383 (San Antonio, TX: NACE 2010).

[8]   M. F. Doerner and W. D. Nix, "A method for interpreting the data from depth-sensing indentation instruments," *J. Mater. Res.*, vol. 1, no. 4, pp. 601−609, Aug. 1986.

[9]   W. C. Oliver and G. M. Pharr, "An improved technique for determining hardness and elastic modulus using load and displacement sensing indentation experiments," *J. Mater. Res.*, vol. 7, no. 6, pp. 1564–1583, Jun. 1992.

[10]   P. J. Burnett and D. S. Rickerby, "The relationship between hardness and scratch adhession," *Thin Solid Films*, vol. 154, no. 1–2, pp. 403–416, Nov. 1987.

[11]   S. J. Bull, "Failure modes in scratch adhesion testing," *Surf. Coatings Technol.*, vol. 50, no. 1, pp. 25–32, Jan. 1991.

[12]   P. Benjamin and C. Weaver, "Measurement of Adhesion of Thin Films," *Proc. R. Soc. A Math. Phys. Eng. Sci.*, vol. 254, no. 1277, pp. 163–176, Feb. 1960.

[13]   C. Weaver, "Adhesion of thin films," *J. Vac. Sci. Technol.*, vol. 12, no. 1, pp. 18–25, Jan. 1975.

[14]   B. Ollivier and A. Matthews, "Adhesion of diamond-like carbon films on polymers: an assessment of the validity of the scratch test technique applied to flexible substrates," *J. Adhes. Sci. Technol.*, vol. 8, no. 6, pp. 651–662, Jan. 1994.

[15]   E. Anyanwu, "Development and Characterization of a New Corrosion Test Set-up Enabling Controlled Water Chemistry and Representative Flow Conditions," in publication 2019.

[16]   "Mechanical Tester For Mechanical Properties Testing." [Online]. Available: https://nanovea.com/mechanical-testers/. [Accessed: 16-Jul-2018].

[17]   N. A. Sakharova, J. V. Fernandes, J. M. Antunes, and M. C. Oliveira, "Comparison between Berkovich, Vickers and conical indentation tests: A three-dimensional numerical simulation study," *Int. J. Solids Struct.*, vol. 46, no. 5, pp. 1095–1104, Mar. 2009.

[18]   W. H. Jiang and R. Kovacevic, "Feasibility study of friction stir welding of 6061-T6 aluminium

alloy with AISI 1018 steel," *Proc. Inst. Mech. Eng. Part B J. Eng. Manuf.*, vol. 218, no. 10, pp. 1323–1331, 2004.

[19]   J. Ning, Y. Zheng, B. Brown, D. Young, and S. Nesic, "Construction and Verification of Pourbaix Diagrams for Hydrogen Sulfide Corrosion of Mild Steel," *CORROSION/2015* paper no. 5507 (Dallas, TX: NACE 2015).